The Correction of Measured Neutron Structure Factors for Thermal Diffuse Scattering

By B. T. M. Willis

Atomic Energy Research Establishment, Harwell, England

To calculate the magnitude of the correction of measured neutron structure factors for thermal diffuse scattering, it is necessary to know the ratio of the sound velocity in the crystal, c_s, to the neutron velocity, v_n. For $\beta(=c_s/v_n) < 1$, the correction is independent of v_n and is evaluated using exactly the same procedure as for X-ray structure factors. For $\beta > 1$, the correction depends on v_n and requires a more complicated analysis than for X-rays, although under certain conditions (discussed in the text) there is no correction at all to the measured intensities. Accurate neutron structure factor measurements are conveniently made with neutrons which are faster than the maximum sound velocity in the crystal; for a 'soft' material such as lead this condition implies that the neutron wavelength does not exceed 1·70 Å, whereas for tungsten, a 'hard' material, the upper limit is 0·77 Å.

1. Introduction

The correction of measured X-ray intensities for thermal diffuse scattering (TDS) has been discussed in a number of recent papers [see Cochran (1969) for a review of existing calculations]. We consider here the theory for making the corresponding correction in neutron diffraction. Much of this theory can be taken over directly from the X-ray treatment, and so we shall deal only with the part where the two treatments diverge. The ratio c_s/v_n, where c_s is the velocity of sound in the sample and v_n is the velocity of the scattered neutrons, plays a critical role in the neutron theory.

The influence of TDS on measured neutron intensities has already been considered briefly by Willis (1969), Rouse & Cooper (1969) and Cooper (1970). We shall follow the arguments given in these papers, extending them where necessary.

Our analysis emphasizes the geometrical characteristics of the scattering of neutrons in reciprocal space. [Readers interested in a detailed analytical treatment of the scattering close to the Bragg angle are referred to the papers of Waller & Froman (1952) and Sjölander (1955).] One-phonon scattering only will be considered; two-phonon and higher-order processes will be ignored. We shall assume, as in the X-ray theory of Nilsson (1957) and others, that the acoustic modes of vibration alone cause a peaking of the TDS at reciprocal lattice points and that these modes all possess the same velocity, independent of the directions of propagation and polarization. Thus

$$\omega(\mathbf{q}) = c_s q \qquad (1)$$

where $\omega(\mathbf{q})$ is the circular frequency of the modes with wave-vector $\mathbf{q}$ and the proportionality constant, c_s, is the same for all modes.

In the next section, we describe the topology of the 'scattering surfaces' for the one-phonon scattering of thermal neutrons close to the Bragg angle. These surfaces are defined as the locus of points in reciprocal space which give rise to one-phonon scattering for a fixed wavelength of the incident beam and a fixed orientation of the crystal. The surfaces are very different from the corresponding surface, the Ewald sphere, appropriate to the one-phonon scattering of X-rays. The TDS contribution to the neutron intensity measured at a fixed orientation of the crystal can then be calculated (§ 3) by summing the scattering cross-sections from all the modes lying on the scattering surfaces. The rest of the evaluation of the TDS correction for the particular scan adopted in measuring the Bragg peak is the same as for X-rays. In § 4, we discuss the implications of the present analysis in choosing a suitable neutron wavelength for accurate structure-factor measurements by neutron diffraction.

2. One-phonon scattering surfaces

The coherent one-phonon scattering of neutrons is governed by the conservation laws for momentum transfer

$$\mathbf{Q} \equiv \mathbf{k} - \mathbf{k}_0 = \mathbf{B} + \mathbf{q} \qquad (2a)$$

and for energy transfer

$$\hbar^2(k^2 - k_0^2)/2m_n = -\varepsilon\hbar\omega(\mathbf{q}), \qquad (2b)$$

where $\mathbf{k}$, $\mathbf{k}_0$ are the wave-vectors of the scattered, incident neutrons respectively, $\mathbf{B}$ is the reciprocal lattice vector, and m_n is the neutron mass. The same convention, regarding the magnitude of the vectors in equation (2a), is adopted as that used by Cochran (1963), *i.e.* $k_0 = 2\pi/\lambda$ and $B = 4\pi \sin\theta_B/\lambda$, where λ is the neutron wavelength and θ_B is the Bragg angle. ε in equation (2b) is either +1 or −1: $\varepsilon = +1$ corresponds to phonon creation and a loss in energy of the neutrons after scattering, and $\varepsilon = -1$ corresponds to phonon annihilation and a gain in neutron energy. The reciprocal space vectors in equation (2a) are illustrated in Fig. 1.

Equations (2a) and (2b) determine the topology of the scattering surfaces. In the X-ray case, the phonon energy $\hbar\omega(\mathbf{q})$ is negligible compared with the energy of the X-ray photon; (2b) then reduces to $k = k_0$ and the scattering surface is the Ewald sphere. For neutron scattering, however, $\hbar\omega(\mathbf{q})$ is comparable with the
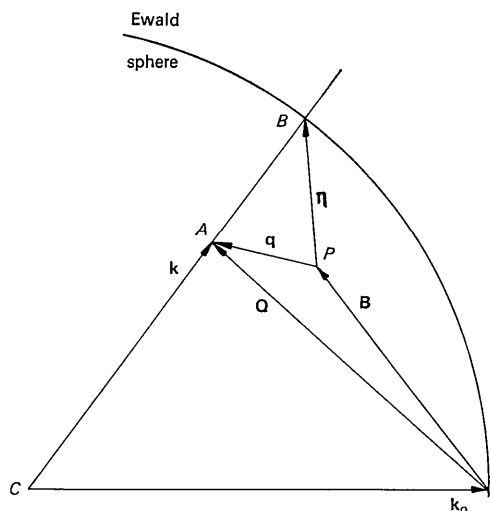

Fig. 1. Vectors in reciprocal space for the one-phonon scattering of neutrons with the creation of a phonon with wavevector q. P is the reciprocal lattice point and A is the endpoint of the wave-vector k of the scattered neutron. The vector AB is $(\varepsilon\hbar\omega/2E)\mathbf{k}$ where E is the neutron energy $(=\hbar^2 k^2/2m_n)$ and ω is the frequency of the mode q. For acoustic phonons, P and A are very close to B; for this reason, the sphere is replaced by its tangent plane at B in later figures.
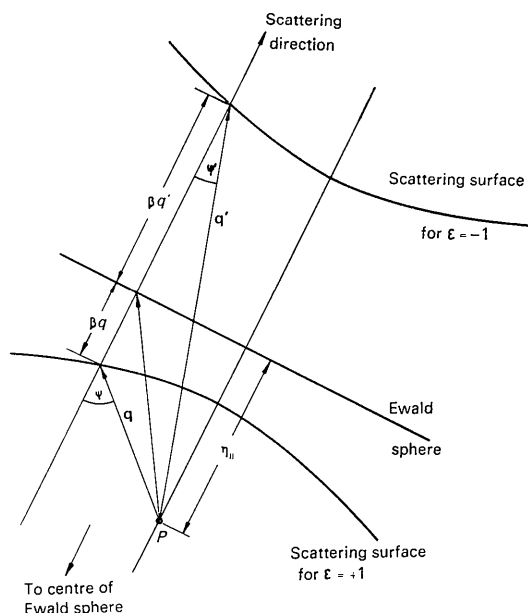

Fig. 2. One-phonon scattering surfaces for $\beta < 1$. The hyperboloid possesses rotational symmetry about the axis CP joining the centre C of the Ewald sphere and the reciprocal lattice point P.

energy of a thermal neutron; thus $k \neq k_0$ and, even though k is not very different from k_0 for scattering by acoustic phonons, the topology of the scattering surfaces is more complicated than for X-rays.

To evaluate the TDS correction for neutrons, we need to discuss the scattering surfaces for one-phonon scattering at crystal settings close to the Bragg angle. The correction is associated with one-phonon processes involving acoustic modes with wave numbers q which are much smaller than the radius k_0 of the Ewald sphere. Using equation (1), equation (2b) reduces for these modes to the approximate form

$$k - k_0 = -\varepsilon\beta q \qquad (3)$$

where $\beta = c_s/v_n$ and $v_n = \hbar k/m_n$. Furthermore, because $q \ll k_0$, we can replace the sphere in the neighbourhood of the reciprocal lattice point by its tangent plane normal to the scattering direction k. Equation (3) then shows that the locus in reciprocal space of the end point of $\mathbf{q}$ is a conic with eccentricity $1/\beta$ (Seeger & Teller, 1942).

For $\beta < 1$, (3) represents a rotational hyperboloid of two sheets with the reciprocal lattice point P at one focus, Fig. 2. There is rotational symmetry about a line through P and normal to the Ewald sphere. The two sheets lie on opposite sides of the Ewald surface (defined by $k = k_0$), so that scattering from q vectors lying on one sheet corresponds to phonon creation $(\varepsilon = +1, k < k_0)$ and scattering from the other sheet to phonon annihilation $(\varepsilon = -1, k > k_0)$. Along a given scattering direction, both processes take place simultaneously: this is illustrated by Fig. 2 where the wavevector q is associated with the phonon creation process and q′ with phonon annihilation.

Fig. 3 shows scattering surfaces for neutrons with twice the velocity of sound, plotted for equal increments of the quantity $\eta_\parallel$. $\eta_\parallel$ is the projection of the vector η along the scattering direction k, where η joins the reciprocal lattice point P and the point of intersection B of the scattering direction and the Ewald sphere (see Fig. 1). $\eta_\parallel$ is a measure of the angle of offset $\Delta\theta$ from the Bragg position:

$$\eta_\parallel = |\mathbf{B}| \cos \theta_B . \Delta\theta = \frac{2\pi}{\lambda} \sin 2\theta_B . \Delta\theta . \qquad (4)$$

Thus in scanning across a reflexion by $\pm 2°$, the maximum value of $\eta_\parallel$ is about one-thirtieth of the radius of the Ewald sphere; the scattering surfaces change continuously in the way illustrated in Fig. 3 throughout the scanning range $2 > \Delta\theta > 0°$, and for the range $0 > \Delta\theta > -2°$ pass through the configurations obtained by reflecting Fig. 3 in the Ewald surface.

For $\beta > 1$, the scattering surface is a rotational ellipsoid with the reciprocal lattice point P at one focus (see Fig. 4). Again there is rotational symmetry about a line through the reciprocal lattice point and perpendicular to the Ewald sphere. The ellipsoid lies wholly on one side or other of the Ewald sphere, depending on which side P is. In contrast to the faster-than-sound

case, the one-phonon scattering takes place for a given orientation of the crystal either by phonon creation or by phonon annihilation, but not by both. Fig. 5 shows scattering surfaces for neutrons with half the velocity of sound and for the same range of $\eta_\parallel$ as that adopted in plotting Fig. 3.

3. Evaluation of TDS correction

At each point in the scan across the Bragg reflexion, the total one-phonon intensity which enters the window of the detector must be calculated. Knowing the dependence of this total intensity on the off-set angle $\Delta\theta = \theta - \theta_B$, the TDS correction can then be evaluated. The complete procedure for evaluating the correction for X-rays is described by Cochran (1969); there are only two steps in this procedure [(a) and (b) below] which are different for neutrons.

(a) The formula giving the cross section for scattering of X-rays by the mode $\mathbf{q}$

$$\left(\frac{d\sigma(\mathbf{q})}{d\Omega}\right)^{(1)} = \frac{NQ^2}{m} \frac{k_BT}{\omega^2(\mathbf{q})} F(\mathbf{Q})^2 \qquad (5)$$

must be replaced by the corresponding formula for neutron scattering:

$$\left(\frac{d\sigma(\mathbf{q})}{d\Omega}\right)^{(1)} = \frac{NQ^2}{2m} \frac{k}{k_0} k_BT \, F(\mathbf{Q})^2 \frac{1}{|J|} \frac{1}{\omega^2(\mathbf{q})} \qquad (6)$$

(see Cochran, 1963; Willis, 1969). $\left(\dfrac{d\sigma(\mathbf{q})}{d\Omega}\right)^{(1)}$ is the

flux of X-rays or neutrons scattered into unit solid angle in a one-phonon process by the mode $\mathbf{q}$, N is the number of unit cells in the crystal, each of mass m, k_B is Boltzmann's constant and T the absolute temperature. For scattering near the Bragg position the magnitude of the scattering vector $\mathbf{Q}$ is $4\pi \sin \theta_B/\lambda$; $F(\mathbf{Q})$ is the structure factor for Bragg scattering. J is a Jacobian term which arises in integrating the one-phonon intensities over all energy transfers. The significance of J was first emphasized by Waller & Froman (1952), who derived the expression

$$J = 1 + \varepsilon\beta q_\parallel/q \qquad (7)$$

where $q_\parallel$ is the projection of $\mathbf{q}$ along the scattering direction $\mathbf{k}$.

· (b) In applying formula (6), the end-point of $\mathbf{q}$ must be restricted to the neutron scattering surface (§ 2), whereas in using formula (5) for X-rays the end-point of $\mathbf{q}$ lies along the Ewald sphere.

3.1 Faster-than-sound neutrons ($\beta < 1$)

Putting $\omega(\mathbf{q}) = c_s q$ in equation (6) and summing over the cross-sections for phonon creation (mode $\mathbf{q}$) and annihilation (mode $\mathbf{q}'$), the one-phonon intensity in the scattering direction is

$$\left(\frac{d\sigma}{d\Omega}\right)^{(1)} = \frac{NQ^2}{2m} \frac{k}{k_0} k_BT \, F(\mathbf{Q})^2$$

$$\times \left[\frac{1}{|J_{+1}|} \frac{1}{c_s^2 q^2} + \frac{1}{|J_{-1}|} \frac{1}{c_s^2 q'^2}\right]. \qquad (8)$$
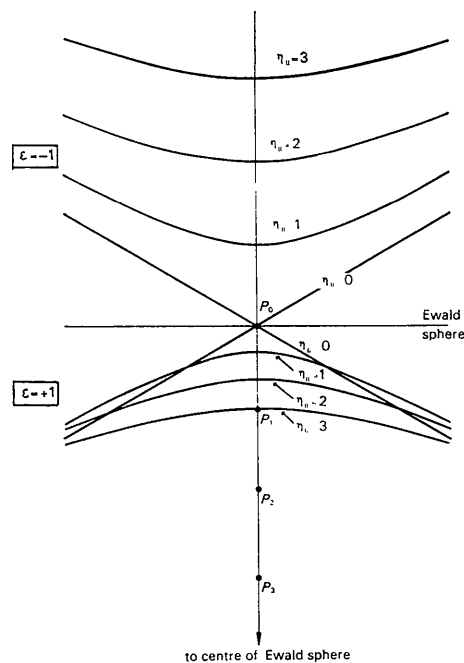

Fig. 3. Faster-than-sound scattering surfaces drawn for $\beta = \frac{1}{2}$ and for equal increments of $\eta_\parallel$, the distance of the reciprocal lattice point P from the Ewald surface. $P_0, P_1, P_2 \ldots$ are the positions of P for $\eta_\parallel = 0, 1, 2 \ldots$.
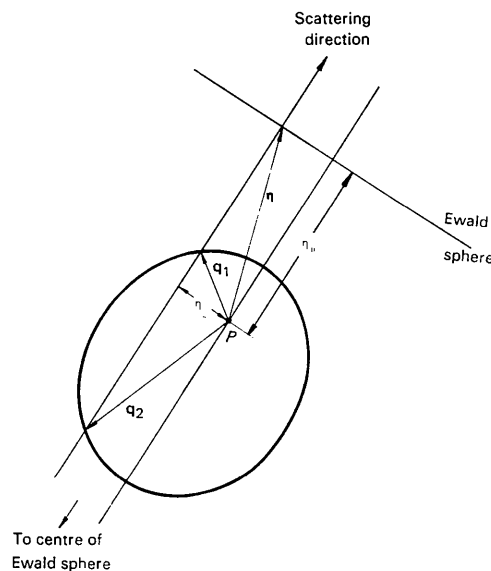

Fig. 4. One-phonon scattering surface for $\beta > 1$, corresponding to processes involving phonon creation. (For phonon annihilation, the reciprocal lattice point P is on the opposite side of the Ewald sphere.) The ellipsoid possesses rotational symmetry about the axis joining P and the centre of the Ewald sphere.

The subscripts on the Jacobians refer to the value of ε: from equation (7)

$$|J_{+1}| = 1 + \beta \cos \psi$$

and $|J_{-1}| = 1 - \beta \cos \psi'$

where ψ, ψ' are the angles illustrated in Fig. 2. Using the geometrical relationships in Fig. 2, the expression in square brackets in equation (8) reduces to

$$\frac{2}{c_s^2 \eta^2} \, ,$$

where η is the wave vector terminating on the Ewald sphere (see Fig. 1). Moreover, for scattering close to the Bragg angle, $k \simeq k_0$ so that (8) becomes

$$\left(\frac{d\sigma}{d\Omega} \right)^{(1)} = \frac{NQ^2}{m} k_B T \, F(\mathbf{Q})^2 \frac{1}{c_s^2 \eta^2} \, . \tag{9}$$

Thus we have obtained the remarkable result that the one-phonon intensity for faster-than-sound neutrons is given by exactly the same formula as for X-rays, equation (5). The neutrons are scattered in the direction $\mathbf{k}$ by the modes $\mathbf{q}$ and $\mathbf{q}'$, but the sum of the intensities from these two processes is the same as if scattering had taken place in the same direction from the mode η which is operative in the X-ray case.

We conclude, therefore, that the TDS correction for faster-than-sound neutrons is evaluated using the same formulae as for X-rays (see Cochran, 1969). This result is at variance with that given by Rouse &

Fig. 5. Slower-than-sound scattering surfaces drawn for $\beta = 2$ and for equal increments of η_1, the distance of the reciprocal lattice point P from the Ewald surface. $P_0, P_1, P_2 \ldots$ are the positions of P for $\eta_1 = 0, 1, 2 \ldots$.

Cooper (1969) (who state that the neutron and X-ray formulae are only identical in the limit, $\beta \to 0$) because of an error later noted by these authors (Rouse & Cooper, 1970) in their analysis.

3.2 Slower-than-sound neutrons ($\beta > 1$)

We have seen in § 2 that for slower-than-sound neutrons the scattering surface encloses the reciprocal lattice point; the one-phonon scattering is confined, therefore, to a diffuse region surrounding the reciprocal lattice point, and there is no scattering for directions $\mathbf{k}$ lying outside this region (Lowde, 1954). This situation contrasts with that for faster-than-sound neutrons where the scattering surface extends across the whole of the Brillouin zone. It is clear from Fig. 5 that the size of the diffuse region increases with $\eta_\parallel$ or with the off-set angle $\Delta\theta$: if $\Delta\varphi$ is the semi-angle subtended by the ellipsoid at the centre C of the Ewald sphere, then it is readily shown that

$$\Delta\varphi = (\beta^2 - 1)^{1/2} \sin^2 \theta_B \, . \, \Delta\theta \, . \tag{10}$$

What is the effect of the TDS on the measured Bragg intensity if the scattering from the whole of the diffuse region enters the detector at each position in the scan across the Bragg peak? To answer this we must calculate the TDS intensity arising from all the modes with wave-vectors $\mathbf{q}$ which terminate on the scattering surface. This calculation is given in the Appendix and leads to an equation which shows that the total intensity is *independent* of the deviation from the Bragg setting. As the reciprocal lattice point approaches the Ewald sphere, the scattering surface contracts (see Fig. 5) and fewer modes contribute to the scattering; however, the contribution from each mode, proportional to q^{-2}, increases, and the two effects exactly counterbalance one another. Consequently, there is no peaking of the TDS at the Bragg position: all the TDS is subtracted off by making a background measurement on either side of the Bragg peak, and so there is *no* TDS correction. This then leads us to enquire into the condition for all the one-phonon scattering to enter the detector.

This condition is dependent on the type of scan adopted in measuring the reflexion. Fig. 6 is a diagram in reciprocal space showing the direction of scanning across the diffuse region enclosing the reciprocal lattice point, for different types of scan. The major axis of the rotational ellipsoid representing the diffuse region lies along the radial direction joining the reciprocal lattice point P to the centre C of the Ewald sphere. At low Bragg angles in the $\theta - 2\theta$ scan and at the limit the scan the detector may 'see' no TDS at all, because for all $\mathbf{k}$ vectors entering the detector the minimum deviation of $\mathbf{k}$ from the radial direction CP may exceed the semi-angle $\Delta\varphi$ subtended by the diffuse region at C. As $\mathbf{k}$ moves from inside to outside the diffuse region, there will be a discontinuity in the TDS intensity. [This type of discontinuity has been discussed
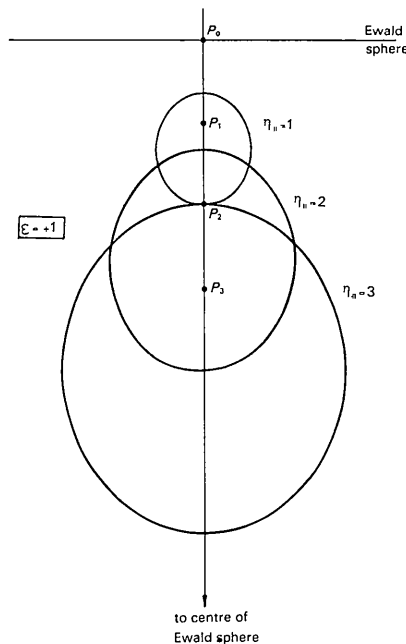
further by Waller & Froman (1952) and Sjølander (1955).]

For the purpose of measuring accurate structure factors using slower-than-sound neutrons, it is preferable to avoid such a discontinuity. This can be done by adopting a *radial scan*, for which the detector window is centrally aligned along CP for all values of θ, in scanning across the Bragg peak. The radial scan requires a rather complicated coupling of the angular movements of crystal and detector. If the crystal movement is $\pm\Delta\omega$ and the detector movement is $\pm 2\Delta\theta$, then $\Delta\omega$: $2\Delta\theta = 1:2 \sin^2 \theta$. (At $\theta_B = 0$ the radial scan is equivalent to an ω scan, and at $\theta_B = 90°$ to a $\theta - 2\theta$ scan.) The condition for all the TDS intensity to enter the window in a radial scan is

$$\Delta\alpha \geq \Delta\varphi \qquad (11)$$

where $\Delta\alpha$ is the semi-angle subtended by the width of the window at the crystal. From equation (10) this condition is readily met for low-angle ($\theta_B \simeq 0$) and for high-angle ($\theta_B \simeq 90°$) reflexions, but for intermediate reflexions equation (11) sets a lower limit to the magnitude of β for slower-than-sound neutrons. For β slightly greater than unity, the diffuse scattering occurs over a volume of reciprocal space which may be larger than that encompassed by the detector and so a finite TDS correction is required. For the ω scan and the $\theta - 2\theta$ scan, the range of β requiring a TDS correction is larger. Clearly, the calculation of the correction will be less straightforward than for faster-than-sound neutrons.

We conclude that for slower-than-sound neutrons there is no TDS correction provided that β is not too close to unity, but the 'forbidden' range of β depends on the Bragg angle θ_B and on the type of scan adopted in measuring the reflexions. This conclusion is an extension of the one given earlier (Willis, 1969) that, to a first approximation, there is no TDS correction for the scattering of slower-than-sound neutrons.

4. Discussion

We have treated the simplest case, originally considered by Nilsson (1957) for X-rays, in which all acoustic modes of vibration have the same velocity. This assumption is not even valid for elastically isotropic crystals, which have *two* distinct velocities (longitudinal and transverse). However, it can be shown (Sjølander, 1955) that, for the more realistic case of two sound velocities, the same formula again describes the one-phonon intensity for both neutrons and for X-rays scattered near the Bragg angle, provided that the neutrons are faster than *both* sound velocities. [This formula is simply equation (9) with c_s^2 replaced by $\frac{1}{3}(c_l^2 + 2c_t^2)$, where c_l and c_t are the longitudinal and transverse sound velocities.] This means, therefore, that no modification is required to the conclusions arrived at in § 3.1 regarding the scattering of faster-than-sound neutrons.

Similarly, we expect that a detailed analysis of the two-velocity model will not affect the conclusion, given in § 3.2, that there is no TDS correction for the scattering of slower-than-sound neutrons, provided that the whole of the TDS enters the detector during the measurement scan. We have discussed the implications of this proviso above, but we have made no attempt to calculate the magnitude of the correction (which will be less than that given by the X-ray formulae) if the proviso cannot be met.

It is apparent from our analysis that the TDS correction is made most easily by choosing a sufficiently short neutron wavelength to ensure that the neutron velocity exceeds the maximum sound velocity in the crystal: the procedure for making the correction is then exactly the same as for X-rays. This wavelength is 0·92 Å for barium fluoride and 1·13 Å for hexamethylenetetramine, two materials which have been examined recently at Harwell by neutron diffraction. The critical wavelength for other materials is readily calculated from a knowledge of their elastic constants: for tungsten, which is a hard material, it is 0·77 Å and for lead, a soft material, it is 1·70 Å.

A corollary of the present study is that time-of-flight measurements of Bragg intensities are less satisfactory than conventional measurements conducted at a fixed neutron wavelength. In the time-of-flight technique (Turberfield, 1970), the different reflecting planes select different wavelengths from the incident 'white' beam; thus the ratio c_s/v_n varies appreciably from one family of planes to another, and the TDS correction will be very difficult to determine, especially for those planes with c_s/v_n slightly greater than unity.
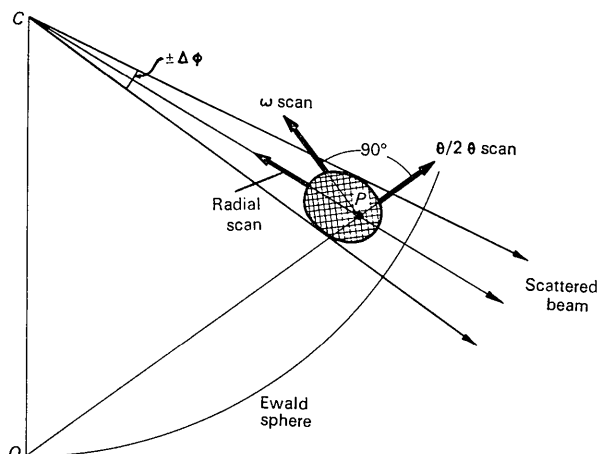
Fig. 6. Diagram showing directions of scanning in reciprocal space for three types of scan: ω scan, $\theta-2\theta$ scan and radial scan. The cross-hatched area represents the diffuse region spanned by those modes involved in the scattering of slower-than-sound neutrons.

APPENDIX

Total TDS intensity for
slower-than-sound neutrons ($\beta > 1$)

Referring to Fig. 4, we need to integrate the differential cross-section $\left(\dfrac{d\sigma(q)}{d\Omega}\right)^{(1)}$ over all modes with wave-vectors q terminating on the surface of the ellipsoid.

Considering first the modes q_1 and q_2 belonging to the same scattering direction k, we find using equation (6) that

$$\frac{d\sigma(q_1)}{d\Omega} + \frac{d\sigma(q_2)}{d\Omega} = \frac{NQ^2}{m} \frac{k_B T}{c_s^2} F(Q)^2 .$$

$$\times \frac{\beta}{\eta^2 \sqrt{1-(\beta^2-1)\,(\eta_\perp/\eta_\parallel)^2}}.$$

Here $\eta_\parallel$, $\eta_\perp$ are the projections of the vector η, joining the reciprocal lattice point to the Ewald sphere, along and perpendicular to the scattering direction. By taking the q vectors in pairs the integration over the ellipsoid is reduced to an integration over a circle of radius R, representing the projection of the ellipsoid on the Ewald plane. The total one-phonon cross-section for a given setting of the crystal is therefore

$$\sigma_1 = \frac{NQ^2}{m} \frac{k_B T}{c_s^2} F(Q)^2 \int_0^R \frac{\beta}{\eta^2 \sqrt{1-(\beta^2-1)\,(\eta_\perp/\eta_\parallel)^2}} .$$

$$\times\, 2\eta_\perp d\eta_\perp \cdot \frac{1}{k_0^2} .$$

Putting $\sin x = \dfrac{\eta_\perp}{\eta_\parallel} (\beta^2-1)^{1/2}$,

$$\int_0^R \frac{\eta_\perp d\eta_\perp}{\eta^2 \sqrt{[1-(\beta^2-1)\,(\eta_\perp/\eta_\parallel)^2]}} = \frac{1}{\beta} \tanh^{-1}\left(\frac{1}{\beta}\right),$$

so that finally

$$\sigma_1 = \frac{NQ^2}{m} \frac{k_B T}{c_s^2} F(Q)^2\, 2k_0^2 \tanh^{-1}\left(\frac{1}{\beta}\right).$$

Thus σ_1 increases from nothing at very long neutron wavelengths ($\beta \gg 1$) to a maximum at the critical wavelength, $\beta = 1$. It is independent of the deviation, $\Delta\theta$, of the crystal from the Bragg setting.

References

COCHRAN, W. (1963). *Rep. Progr. Phys.* **26**, 1.
COCHRAN, W. (1969). *Acta Cryst.* A**25**, 95.
COOPER, M. J. (1970). *Thermal Neutron Diffraction*, Ch. 4. Edited by B. T. M. WILLIS. Oxford Univ. Press.
LOWDE, R. D. (1952). *Proc. Roy. Soc.* A**221**, 206.
NILSSON, N. (1957). *Ark. Fys.* **12**, 247.
ROUSE, K. D. & COOPER, M. J. (1969). *Acta Cryst.* A**25**, 615.
ROUSE, K. D. & COOPER, M. J. (1970). *Acta Cryst.* A**26**, 457.
SEEGER, R. J. & TELLER, E. (1942). *Phys. Rev.* **62**, 37.
SJØLANDER, A. (1955). *Ark. Fys.* **7**, 375.
TURBERFIELD, K. C. (1970). *Thermal Neutron Diffraction*, Ch. 3. Edited by B. T. M. WILLIS. Oxford Univ. Press.
WALLER, I. & FROMAN, P. O. (1952). *Ark. Fys.* **4**, 183.
WILLIS, B. T. M. (1969). *Acta Cryst.* A**25**, 277.

The Elastic Constants of the Triclinic Crystals Ammonium and Potassium Tetroxalate Dihydrate

By H. KÜPPERS AND H. SIEGERT

Institut für Kristallographie der Universität zu Köln, Germany

In the triclinic crystals ammonium and potassium tetroxalate dihydrate 34 and 31 sound velocities respectively were measured by means of the diffraction of light by ultrasonic waves. From these velocities the 21 independent components of the elastic tensor were calculated. Thus, the method first tested by Haussühl & Siegert on $CuSO_4.5H_2O$ was successfully applied to two other triclinic crystals. The compounds under investigation were found to exhibit an extremely high elastic anisotropy.

Introduction

The elastic behaviour of triclinic crystals is described by a fourth-rank tensor containing 21 independent components. The determination of these 21 constants from measurements of sound velocities involves, apart from a larger experimental expenditure, severe numerical difficulties. Haussühl & Siegert (1969) determined for the first time the elastic constants of a triclinic crystal, $CuSO_4.5H_2O$. It is the aim of the present investigation to apply the method used by Haussühl & Siegert (1969) to other crystals in order to test